Title

Preliminary estimation of seismically induced ground strains from spatially variable ground motions

Authors

Ancheta, Timothy D
Stewart, Jonathan P
Abrahamson, Norman A.
et al.

Publication Date

2008

Peer reviewed

PRELIMINARY ESTIMATION OF SEISMICALLY INDUCED GROUND STRAINS FROM SPATIALLY VARIABLE GROUND MOTIONS

Timothy D. Ancheta[1], Jonathan P. Stewart[2], Norman A. Abrahamson[3], and Robert L. Nigbor[4]

[1]Graduate student researcher, Dept. of Civil & Environmental Engineering, Univ. of Calif. Los Angeles, 5371 Boelter Hall, Los Angeles, CA 90095; tancheta@ucla.edu
[2]Professor and Vice Chair, Dept. of Civil & Environmental Engineering, Univ. of Calif. Los Angeles, 5371 Boelter Hall, Los Angeles, CA 90095; jstewart@seasnet.ucla.edu
[3]Seismologist, PG&E, PO Box 770000, San Francisco, CA 94177; NAA2@pge.com
[4]Researcher, Dept. of Civil & Environmental Engineering, Univ. of Calif. Los Angeles, 5371 Boelter Hall, Los Angeles, CA 90095; nigbor@ucla.edu

ABSTRACT: A model for horizontal peak ground strain (*PGS*) is developed in consideration of three fundamental contributions to spatially variable ground motion (SVGM): (1) spatial incoherence effects, which contribute to phase variability in a stochastic sense; (2) wave passage effects, which contribute to phase variability in a deterministic sense; and (3) amplitude variability. Previous models for each of these effects are reviewed and compared to array data from Borrego Valley, California. Published empirical models for coherency and amplitude variability are found to represent reasonably well the Borrego data. We extend previous work by considering correlations of amplitude and phase variability (generally found to be small) and characterizing the coherency-dependent probabilistic distribution of phase variability. Using the aforementioned amplitude and phase variability models, a procedure is developed to generate simulated acceleration records from a seed record. The procedure is applied to a suite of Northridge earthquake recordings to predict ground strains, which are found to be strongly dependent on the peak ground velocity (*PGV*) of the seed motion and the separation distance between the seed and simulated motions. The dependence of *PGS* on *PGV* saturates for large *PGV* (> 50 cm/sec).

INTRODUCTION

A number of approaches have been described in the literature for characterizing ground strain from strong ground motion. One prevailing approach examines strains along a particular alignment (e.g., a pipeline or tunnel) due to wave passage (e.g., Newmark, 1967). In this approach, peak ground strain (*PGS*) is represented as some fraction of the ratio of peak ground velocity (*PGV*) to shear wave velocity (V_s). The main drawback for this approach is that it does not capture additional sources of spatially variable ground motions (SVGM) including incoherent waves and spatially variable site response. Accordingly, it is often preferred for strains to be inferred from recordings of dense field arrays, in which many SVGM effects are implicitly included. There are two general categories of approaches for doing this. The first approach uses a geodetic technique to infer strains directly from differences in ground displacement histories at adjacent stations O'Rourke et al. (1984), Bodin et al. (1997), Paolucci and

Smerzini (2007), Paolucci and Pitilakis (2007). The second approach, used by this study, uses SVGM models of Fourier amplitude and phase variation in a forward modeling sense to generate a simulated motion from a seed recording. Similar approaches have been used previously by Zerva and Zervas (2002) and Abrahamson (1992b). The simulation of SVGM through analysis of amplitude and phase variability recognizes three fundamental sources of ground motion spatial variability:

1. Variability of phase from wave passage.
2. Random (or stochastic) variability of phase, which is often expressed mathematically by a coherency function.
3. Variability of amplitude, which can be expressed by a standard deviation term.

This paper describes the development of a model to predict *PGS* in consideration of the above sources of SVGM. We evaluate phase and amplitude variability relative to existing models using previously unanalyzed array data from Borrego Valley, California. We then describe the development of new procedures for evaluating simulated ground motions from a seed record. Those procedures are then used to estimate ground strains, and predictive equations for *PGS* are developed and compared to previous work. This paper is a brief synopsis of this work, which is described in more detail by Stewart et al. (2007).

DATA SUMMARY

The Borrego Valley Differential Array (BVDA) is located in the San Jacinto Mountains, 40 km west of the Salton Sea in southern California (Kato et al, 1998). It is situated in the northern portion of the Borrego Valley which is an alluvial flood plain which widens to the south. The BVDA consists of multiple surface and downhole arrays, however only the main linear array recordings are used. The array configuration is shown on Figure 1.

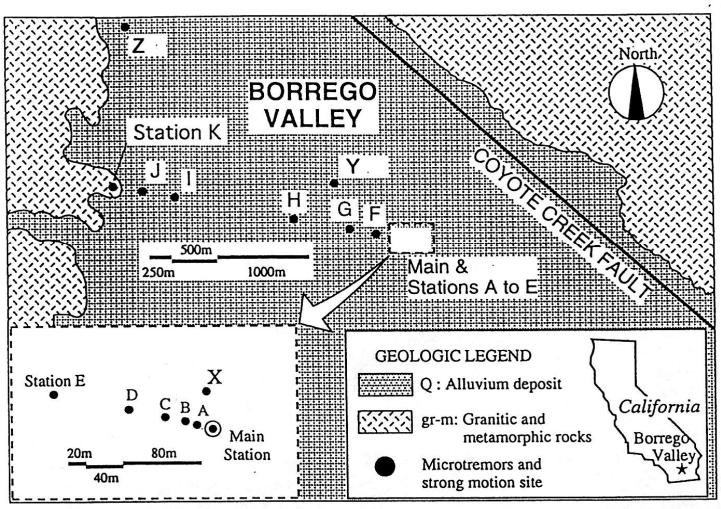

FIG. 1. Plan view of Borrego Valley showing location of BVDA (Kato et al. 1998).

The data was selected from stations 0 (main) and A through E, which are located 10, 20, 40, 60, 80, 160 meters from the main station. The underlying soils consist of medium to very dense coarse to medium grained sands with S-wave velocities of 400 to 600 m/s. The soil overlies a granitic basement located approximately 230 m below the surface with S-wave velocity of greater than 2500 m/s (Kato et al, 1998). From the nearly 200 events recorded, 16 were selected based on a high signal to noise ratio

and minimum 1 sec window length for shear waves to optimize bandwidth. These criteria limit the selected earthquakes to events with M > 2.5, typically with epicentral distances < 80 km.

The array data was pre-processed before application to estimate the coherency and amplitude variability. The S-wave window was identified and used in the analyses. This was done because prior work has shown shear waves to produce larger strains than p-waves or surface waves (e.g., Gupta, 2004). To model the deterministic and stochastic variation separately, the S-wave windows were aligned in time with reference station 0 to remove wave passage effects. After extraction the aligned S-wave signals were tapered in the time domain to minimize errors/bias in subsequent frequency domain analysis.

COHERENCY

Coherency is used to quantify phase variation between two signals. To quantify the random phase variation, we use lagged coherency defined as follows (Abrahamson 1992a):

$$\left|\gamma_{jk}\left(\omega\right)\right| = \left|\frac{S_{jk}\left(\omega\right)}{\left[S_{jj}\left(\omega\right)S_{kk}\left(\omega\right)\right]^{1/2}}\right| \tag{1}$$

where S_{jj} and S_{kk} are the power spectral density functions of stations j and k, S_{jk} is the cross power spectral density function, and ω is the circular frequency (radians/sec). The statistical distribution of lagged coherency data is approximately normal when transformed using a $\tanh^{-1}$ function (Abrahamson 1992a).

Values of lagged coherency are sensitive to the smoothing method that is used (e.g., lagged coherency of unsmoothed records is unity). We smooth the data using an 11-point (M=5) Hamming lag window (Brillinger, 1981; Abrahamson, 1992a), which is a frequency-domain smoothing procedure applied to power spectra. The application of smoothing produces a trade-off between resolution and data scatter – as the level of smoothing increases the scatter of the coherency decreases but the mean value also decreases. Additional justification for the smoothing procedure adopted here is given by Abrahamson (1992a) and Stewart et al. (2007).

Abrahamson (1992a) developed an empirical model for lagged coherency using recordings from the LSST (Large Scale Seismic Test) array in Taiwan. The model takes as input frequency (f) and separation distance (ξ). For large frequencies, the model converges asymptotically to a value of $|\gamma|$=0.35, which corresponds to the lagged coherency of white noise for the selected level of smoothing.

The lagged coherency of the BVDA data is plotted against the Abrahamson (1992a) model in Figure 2. The model generally fits the BVDA data well, although there is bias for frequencies below 10 Hz (under-prediction for ξ=10 m; over-prediction for ξ>10 m).

BVDA data were also used to investigate the distribution of the random phase variation and the correlation between random phase components. This information is

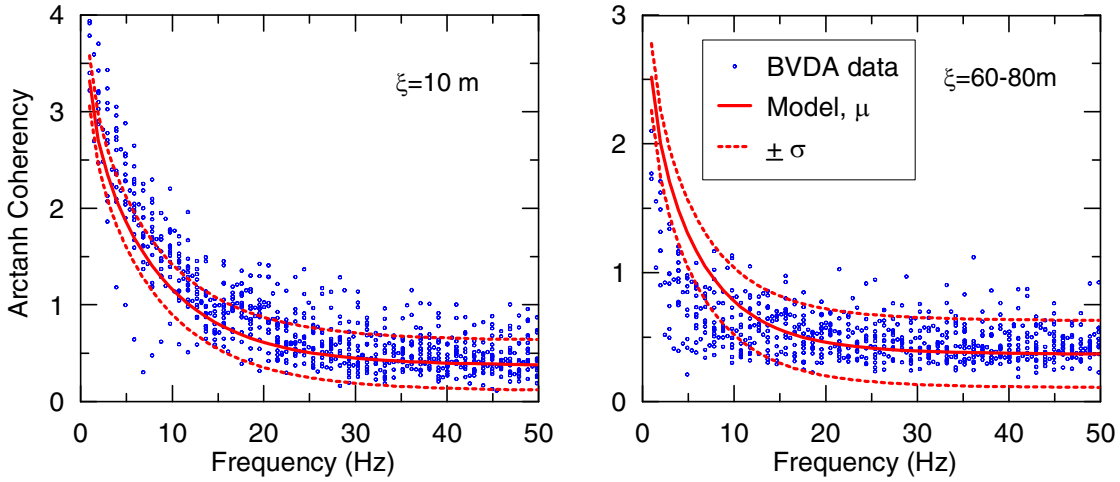

FIG. 2. Transformed lagged coherency data from BVDA plotted again model of Abrahamson (1992a). μ=median; σ=standard deviation.

important for the generation of simulated motions, as described subsequently. Histograms of wrapped phase differences between station pairs are plotted for various frequency bins in Figure 3. The standard deviation terms, $\sigma_{\phi,wr}$, reported in Figure 3 are those of the data with their shown distribution, which appears to be a hybrid of a normal distribution and a uniform distribution (the latter dominating at higher frequencies). However, Stewart et al. (2007) showed that the distributions in Figure 3 are for all practical purposes normal distributions (standard deviation = σ_ϕ) of unwrapped phase differences – in other words, the warping of the tails of the distribution occurs because of wrapping. Because of the effects of wrapping, $\sigma_\phi \geq \sigma_{\phi,wr}$).

As described further in Stewart et al. (2007), correlation coefficients of phase variations from frequency-to-frequency average approximately zero, indicating that variability of wrapped phase angle is essentially random.

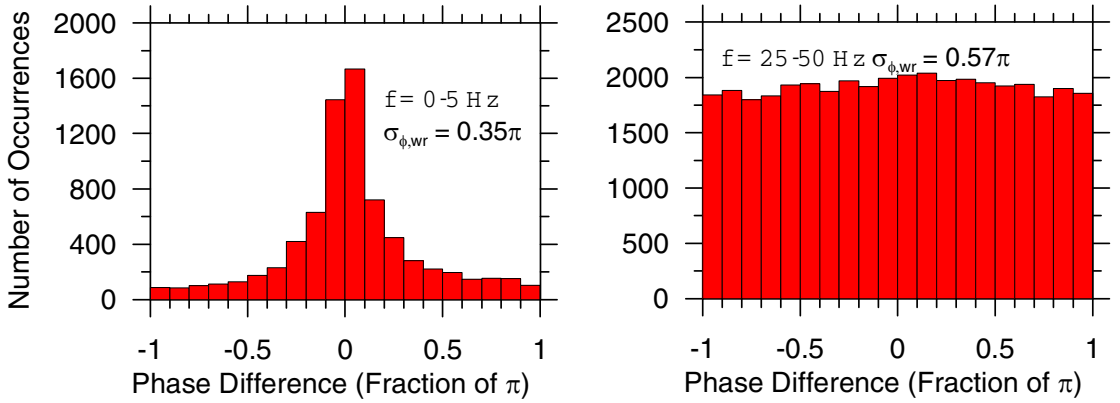

FIG. 3. Histogram of wrapped differences between Fourier Phases from all BVDA station pairs for separate frequency bins as noted.

AMPLITUDE VARIATION

The amplitude variation between two stations is taken as the difference of the natural logs of the Fourier amplitudes and is denoted $\Delta A(f,\xi)$. If a series of values of ΔA are collected, the distribution should have zero mean. The standard deviation of the distribution is denoted $\sigma_{\Delta A}(f,\xi)$. Standard deviation term $\sigma_{\Delta A}$ is calculated using unsmoothed Fourier amplitude spectra so as to be compatible with the procedure for generating simulated ground motions described below.

An empirical function for $\sigma_{\Delta A}(f,\xi)$ has been developed by Abrahamson (2007, personal communication) as follows:

$$\sigma_{\Delta A}(f,\xi) = A\left(1-e^{Bf+C\xi}\right) \tag{2}$$

where A-C are regression parameters with values A=0.93, B=–0.163, and C=–0.0019. This regression was performed using the maximum likelihood method by selecting the best fit line for many different arrays from soil sites (Chiba, Hollister, Imperial Valley Differential Array, LSST).

The model represented by Eq. 2 was compared to BVDA data. Figure 4 shows the model for $\sigma_{\Delta A}$ plotted against data for all of the BVDA selected events. Each blue dot in Figure 4 represents a standard deviation ($\sigma_{\Delta A}$) calculated on all data within the specified separation distance range for a fixed frequency. The results show that amplitude variability is more strongly dependent on frequency than on separation distance and that $\sigma_{\Delta A}$ reaches a limiting value of 0.929 at high frequencies (regardless of separation distance). The fit to the data is generally satisfactory.

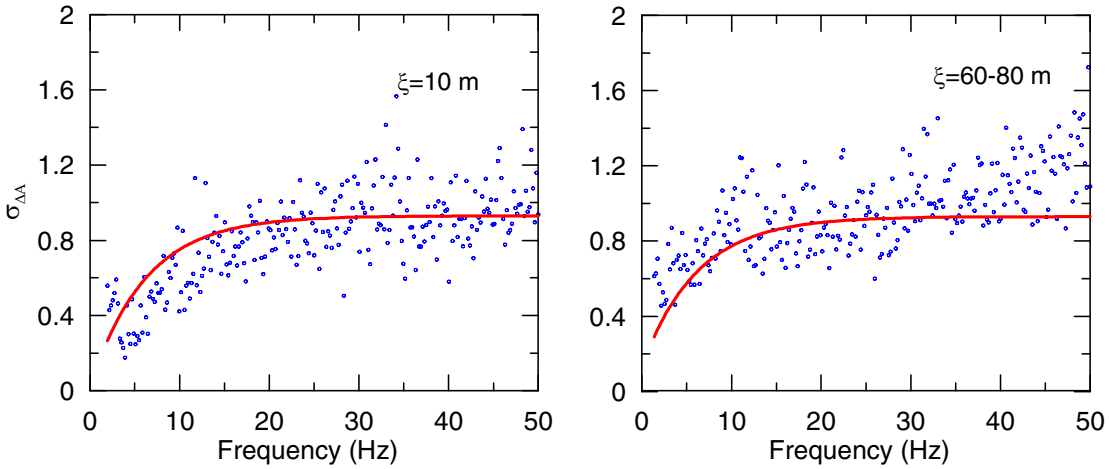

FIG. 4. Plot of $\sigma_{\Delta A}$ from BVDA data compared to model

As described further in Stewart et al. (2007), correlation coefficients of amplitude variability from frequency-to-frequency range from about 0.3 for frequency steps of approximately 0.2 Hz to nearly zero for frequency steps approaching 10 Hz. Correlations between differences of natural logarithms of amplitude and unmodified phase differences at a common frequency were also investigated and found to be nearly zero. Based on these result, we assume amplitude residuals to be uncorrelated with each other and with phase.

GENERATION OF SPATIALLY VARIABLE GROUND MOTIONS

In this section, we describe the process adopted for the generation of a pair of spatially variable ground motions (SVGM). One of the motions is referred to as the "seed" motion and consists simply of an individual recording. The second motion is different from the first as a result of a modification of the phase and amplitude; that motion is referred to as the "simulated" motion. For the development of the strain model herein we assume the new location is oriented in the direction of the wave ray path as we use the full apparent wave velocity with a slowness of S=0.4 sec/km.

Consider a seed motion with phase ϕ_k. The phase of the simulated motion ϕ_j is evaluated by adding a stochastic component ε_{jk} along with the phase shift from wave passage:

$$\phi_j(f) = \phi_k(f,\xi) + \varepsilon_{jk}(f) + 2\pi f \xi S \tag{3}$$

A separate random number ε_{jk} is used for each frequency except the zero frequency component (f=0) because of the lack of correlation of random phase variations across frequencies. Each random number is generated according to a normal distribution with μ=0 and standard deviation=σ_ϕ (i.e., standard deviation of unwrapped phase angles). Term σ_ϕ is related to lagged coherency -- as $|\gamma|$ drops σ_ϕ increases. Stewart et al. (2007) derive the relationship between $|\gamma|$ and σ_ϕ, which is found to follow the relationship shown in Figure 5. The minimum value of 0.33 corresponds to the limiting value of lagged coherency obtained from BVDA data for the selected method of smoothing. After generating a realization of ε_{jk} and adding the phase shift from wave passage per Eq. 3, the modified phase is then wrapped to be within the limits of [-π, π].

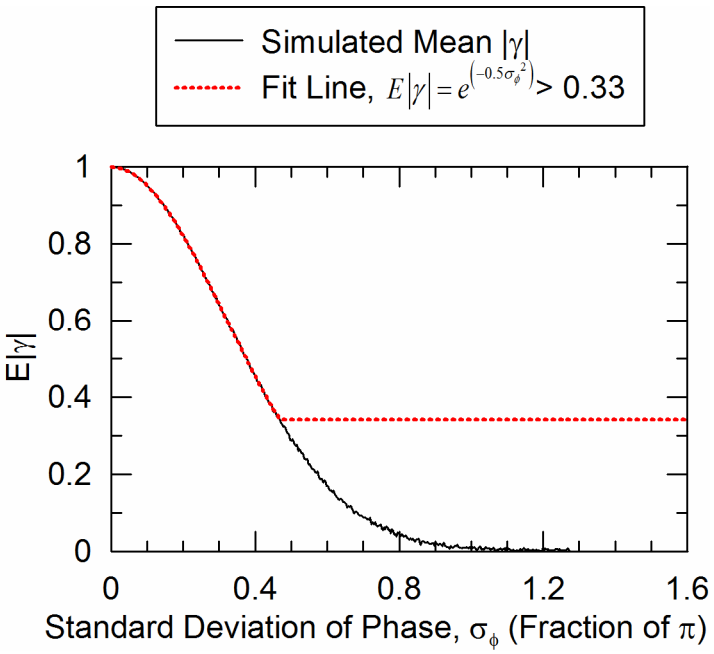

FIG. 5. Relationship between sigma and lagged coherency

As with the phase variation, the Fourier amplitude of the seed motion is modified by adding a stochastic component ε_{jk} as shown below:

$$A_j(f) = \exp\left\{\ln\left[A_k(f)\right] - \varepsilon_{jk}(f)\cdot\frac{1}{\sqrt{2}}\sigma_{\Delta A}(f)\right\} \tag{4}$$

The random numbers for amplitude are generated according to a normal distribution with μ=0 and standard deviation=$\sigma_{\Delta A}$, where $\sigma_{\Delta A}$ is in turn calculated using Eq. 2. Independent random numbers are used for each frequency except the DC-component, which is not modified. The random numbers used for amplitude are independent of those used for phase due to the lack of correlation.

PREDICTION MODEL FOR STRAINS

In this section we develop a predictive model for *P*eak *G*round *S*train (*PGS*). A suite of N_s seed motions is selected from Northridge earthquake recordings with a range of amplitudes. For seed motion *i*, a simulated motion is generated using the procedure given in the above section for a given separation distance ξ. The seed and simulated acceleration are integrated twice to displacement histories. A strain history is calculated as the difference between the seed and simulated displacement histories normalized by ξ. The peak value of strain from the strain history is taken as *PGS*. The simulation procedure is repeated approximately 30 times to generate a suite of *PGS* values for seed motion *i* and separation distance ξ. This is repeated for all N_s seed motions and for a suite of separation distances. Using those results, a prediction equation was developed to estimate *PGS* as a function of separation distance ξ and peak ground velocity (*PGV*).

The seed motions utilized in this work are from stations with NEHERP C and D site categories. One component of motion was arbitrarily selected for each site. All data was taken from the PEER database (http://peer.berkeley.edu/nga/). The selected stations are listed by Stewart et al. (2007).

A baseline correction procedure was developed to minimize the effect of long period noise on *PGS* estimates. The full baseline correction procedure is given by Stewart et al. (2007), but the most important aspect of the procedure is that baseline correction was applied to the differential displacement between the seed and simulated displacements. This avoids the potential for errors associated with inconsistent baseline correction of the two records. We used a baseline correction consisting of a high-order polynomial without constant or slope terms fit to the acceleration-time data. A 10^{th} order polynomial was used; however it was found that the order of the polynomial used was relatively inconsequential to the *PGS* estimates.

Individual estimates of PGS from the Northridge accelerograms are given in Figure 6. Each "column" of points corresponds to the 30 *PGS* estimates for a given record. For a given separation distance (ξ), *PGS* is seen to increase with *PGV* initially, but then to saturate for large *PGV*. This behavior can be captured with a hyperbolic function, as shown by the fit curves in Figure 6. A preliminary model for PGS conditional on PGV and ξ is given by the following expression:

$$PGS = \frac{PGV}{\left(a_1\xi - a_2\xi^2\right) + \left(b_1\xi - b_2\xi^2\right)\cdot PGV \cdot R} \quad (5)$$

where a_1-a_2 and b_1-b_2 represent regression coefficients given in Figure 6. The log-normal standard deviation of the residuals σ_{PGS}=0.72.

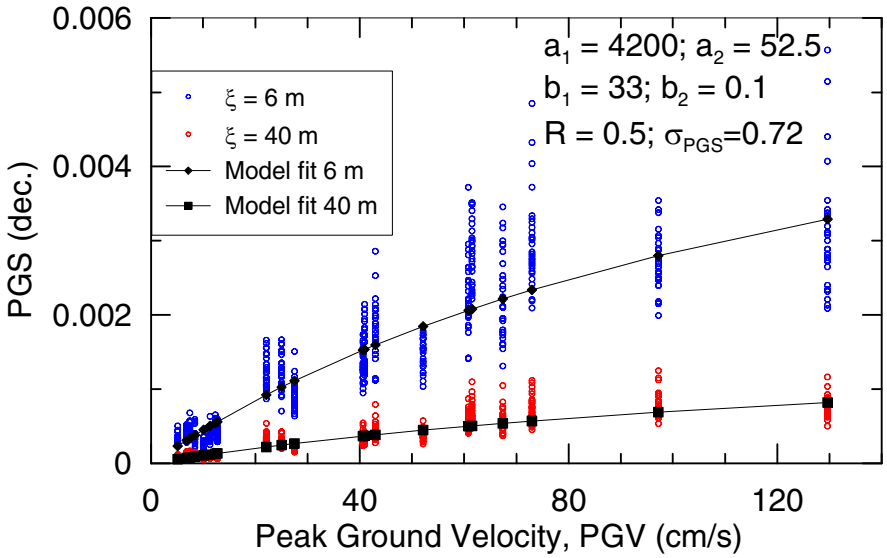

FIG. 6. Plot of model fit to *PGS* data for ξ = 6 m and 40 m

Figure 7 compares strain estimates developed in this study to those from Abrahamson (2003) and Paolucci and Smerzini (2007). Those previous studies parameterized *PGS* in terms of peak displacement (*PGD)*. To facilitate a side-by-side comparison, regression analyses were performed as described above using *PGD* as the intensity measure in lieu of *PGV*. Note that the effect of separation distance was not considered in the previous work. For low *PGD*, the published models pass near the lower bound of our curves, generally being consistent with ξ=24-40 m.

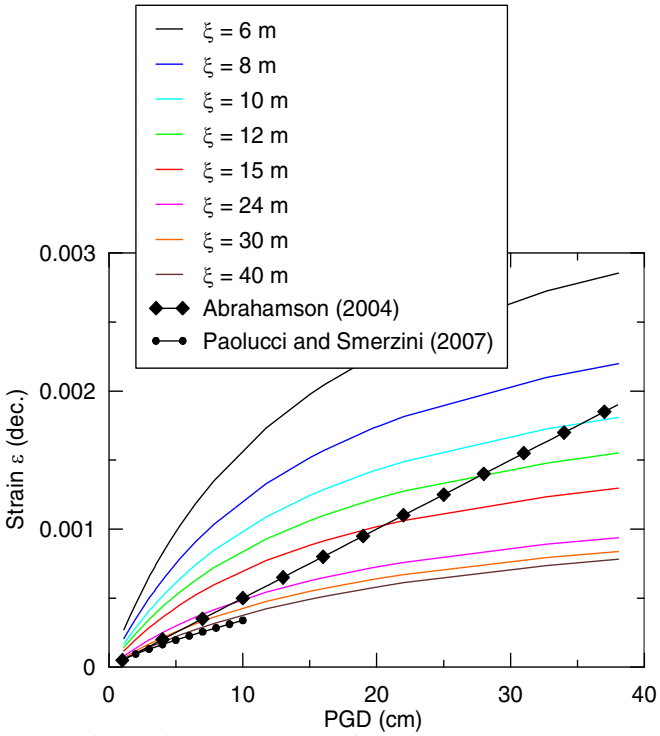

FIG. 7. Comparison of model predictions from present study (colored lines) to

To provide insight that assists in interpreting the trends in the *PGV-PGS* relationship, we identify the frequency range that controls strains. This is done for the Northridge records by exercising the simulated motion generation routine by modifying the coherency and amplitude over a frequency range of zero to a cutoff frequency f_c. Limiting frequency f_c was taken as 0.2%, 1.0%, 2.0%, 10%, 20%, 40%, 60%, 80%, and 100% of the Nyquist frequency (f_{Nyq}). The original procedure takes $f_c = f_{Nyq}$. By successively dropping f_c below f_{Nyq}, we investigate the influence of the different

frequency ranges on ground strains. The results are shown in Figure 8 and indicate that the randomization of frequencies beyond ~4-5 Hz does not appreciably affect strain estimates. Peak strains drop as f_c is dropped across the range of ~0.3 to 4 Hz. These results indicate that components of ground motion in that approximate frequency range control ground strains.

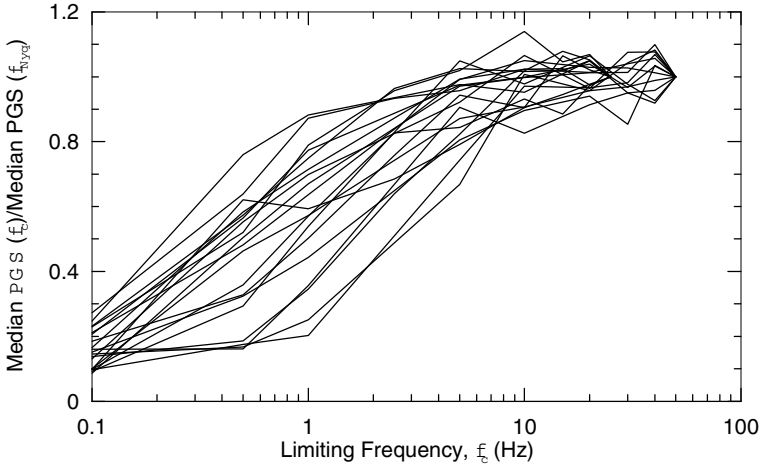

FIG. 8. Variation of PGS with frequency *f* implied by PGS model in Eq. 5.

SUMMARY AND LIMITATIONS

We develop a preliminary model relating peak transient ground strain to peak velocity and separation distance. The model accounts for known sources of spatially variable ground motion including wave passage, incoherent waves, and differential site response, at least to the extent that those effects are captured in the underlying models for coherency and amplitude variability. Those underlying models were developed from relatively weak motion data (PGV < 30 m/s) and an inherent assumption associated with the procedure used here is that the coherency and amplitude variability models apply for larger shaking amplitudes as well. Validation of the computed strains against strains directly inferred from array data is being completed at present.

Our preliminary model is considered applicable to stiff soils sites, separation distances of ξ=6-85 m, and $PGV \leq 120$ cm/sec. The *PGS* model is developed using ground motion recordings from only one event, hence possible effects of magnitude have not yet been investigated. Major new features of this model relative to previous work are the saturation of strain at high PGV and the dependence on ξ.

ACKNOWLEDGEMENTS

This work was supported by Subcontract No. 14 between UCLA and the Consortium of Universities for Research in Earthquake Engineering. This support is gratefully acknowledged. The helpful suggestions of Drs. Brian McDonald and John Osteraas of Exponent and Professor Jonathan Bray of UC Berkeley are appreciated.

REFERENCES

Abrahamson, N.A. (1992a). "Spatial variation of earthquake ground motion for application to soil-structure interaction," *Rpt. No. EPRI TR-100463*, Electrical Power Research Institute, Palo Alto, CA, March.

Abrahamson, N.A. (1992b). "Generation of spatially incoherent strong motion time histories," *Proc. 10th World Conf. Earthquake Engineering*, Vol. II, 845-850.

Abrahamson, N.A. (2003). "Model for strains from transient ground motions," in *CUREE Publication No. EDA-04*, Consortium of Universities for Research in Earthquake Engineering, Richmond, CA, pp 43-79.

Bodin, P., Gomberg, J., Singh, S.K., and Santoyo, M.A. (1997). "Dynamic deformations of shallow sediments in the Valley of Mexico: Part I: Three dimensional strains and rotations recorded on a seismic array," *Bull. Seism. Soc. Am.*, 87, 528-539.

Brillinger, D.R. (1981). *Time series data analysis and theory*, Expanded Edition, Holden Day, San Francisco, CA.

Gupta, A., editor (2004). *Workshop Proceedings: Effects of Earthquake-Induced Transient Ground Surface Deformations on At-Grade Improvements*, CUREE Publication No. EDA-04, Richmond, CA.

Kato, K., Takemura, M., Konno, T., Uchiyama, S., Iizuka, S. and Nigbor, R.L. (1998). "Borrego Valley downhole array in southern California: Instrumentation and preliminary site effect study," *Proc. 2nd Int'l Symposium on the Effects of Surface Geology on Seismic Motion*, Yokohama, Japan.

Newmark, N.M. (1968). "Problems in wave propagation in soil and rock," *Proceedings of the International Symposium on Wave Propagation and Dynamic Properties of Earth Materials*, Albuquerque, NM.

O'Rourke, M.J. Castro, G., and Hossain, I. (1984). "Horizontal soil strain due to seismic waves," *J. Geotech. Engrg.*, ASCE, 110 (9), 1173-1187.

Paolucci, R. and Pitilakis, K. (2007). *Chapter 18: Seismic Risk Assessment of Underground Structures Under Transient Ground Deformation*, Earthquake Geotechnical Engineering, 4th International Conference on Earthquake Geotechnical Engineering – Invited Lectures, K. Pitilakis (editor), 433-459.

Paolucci, R. and Smerzini, C. (2007). "Earthquake induced transient ground strains from dense seismic networks," *Earthquake Spectra*. In review.

Stewart, J.P., Ancheta, T.D., Nigbor, R.L., Bray, J.D., Mason, H.B., Bernardini, J.A., Abrahamson, N.A., and McDonald, B. (2007). "Ground strains from strong ground motion: preliminary empirical characterization and effect on shallow foundations," Report to CUREE. September.

Zerva, A. and Zervas, V. (2002). "Spatial variation of seismic ground motions: an overview," *App. Mech. Rev.*, 55 (3), 271-297.